

Two dark matter candidates: the case of inert doublet and singlet scalars

Ali Mjallal

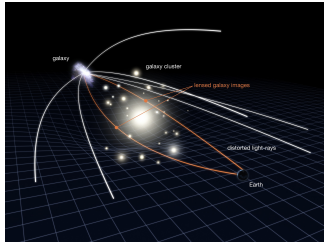
based on [arXiv:2108.08061](#) done by G. Belanger, A. Mjallal, A. Pukhov and submitted to PRD

LAPTh, Annecy

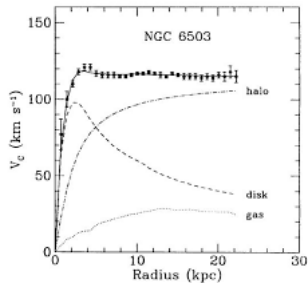
IRN Terrascale Clermont-Ferrand, November 24, 2021

Evidence For Dark Matter

Gravitational Lensing



Galaxy rotation curves



Cosmic Microwave Background (CMB)

The Planck experiment has measured **precisely** the anisotropies in the temperature of the CMB and has determined the relic density of Dark Matter:

$$\Omega_{DM} h^2 = 0.1198 \pm 0.0012$$

Motivation:

The hypothesis that dark matter (DM) is a weakly interacting massive particle (WIMP) has been studied carefully. Experimental searches have probed a vast range of the parameter space for typical WIMP models with no confirmed signal of DM.

We investigate the phenomenology of a specific two-component dark matter model, the inert doublet and singlet model (IDSM).

- The model
- Dark matter relic density and interactions between dark sectors
- Constraints
- Results
 - General scan
 - Nearly degenerate doublet
- Conclusion

The model

- The model is an extension of the SM.
- Minimal scalar Dark Matter model with an extra doublet \tilde{H}' and a complex Singlet \tilde{S} .
- \tilde{H}' has hypercharge 1/2 while \tilde{S} has zero hypercharge.
- We assume that all SM particles are invariant under a discrete \mathbb{Z}_4 symmetry while the inert doublet and singlet have different charges.
- A field ϕ transforms under a discrete \mathbb{Z}_4 symmetry as $\phi \rightarrow \exp\left(i\frac{\pi}{2}X_\phi\right)\phi$, where X_ϕ is the charge of the field ϕ under \mathbb{Z}_4 .

Note that: $\tilde{H}' = \begin{pmatrix} -i\tilde{H}^+ \\ \frac{\tilde{H} + i\tilde{A}}{\sqrt{2}} \end{pmatrix}; X_{\tilde{H}'} = 2 \quad \tilde{S} = \frac{\tilde{S}_H + i\tilde{S}_A}{\sqrt{2}}; X_{\tilde{S}} = 1.$

$$X_{SM} = 0$$

- The first dark sector contains the complex singlet while the 4 particles of the inert doublet belong to the second dark sector.
- Only SM Higgs doublet (H) develops a vacuum expectation value that spontaneously breaks $SU(2) \times U(1)$, $\langle H \rangle = v/\sqrt{2}$ with $v = 246\text{GeV}$.
- \mathbb{Z}_4 symmetry is not broken, therefore \tilde{H}' and \tilde{S} do not couple to fermions.

The model

The scalar potential that satisfy all the above conditions is:

$$\begin{aligned} V_{Z_4} = & \lambda_1 \left(|H|^2 - \frac{v^2}{2} \right)^2 + \mu_2^2 |\tilde{H}'|^2 + \lambda_2 |\tilde{H}'|^4 + \mu_S^2 |\tilde{S}|^2 + \lambda_S |\tilde{S}|^4 \\ & + \frac{\lambda'_S}{2} (\tilde{S}^4 + \tilde{S}^{\dagger 4}) + \lambda_{S1} |\tilde{S}|^2 |H|^2 + \lambda_{S2} |\tilde{S}|^2 |\tilde{H}'|^2 \\ & + \lambda_3 |H|^2 |\tilde{H}'|^2 + \lambda_4 (H^\dagger \tilde{H}') (\tilde{H}'^\dagger H) \\ & + \frac{\lambda_5}{2} \left[(H^\dagger \tilde{H}')^2 + (\tilde{H}'^\dagger H)^2 \right] + \frac{\lambda_{S12}}{2} (\tilde{S}^2 H^\dagger \tilde{H}' + \tilde{S}^{\dagger 2} \tilde{H}'^\dagger H) \\ & + \frac{\lambda_{S21}}{2} (\tilde{S}^2 \tilde{H}'^\dagger H + \tilde{S}^{\dagger 2} H^\dagger \tilde{H}') \end{aligned}$$

The scalar sector of the model has 13 independent parameters

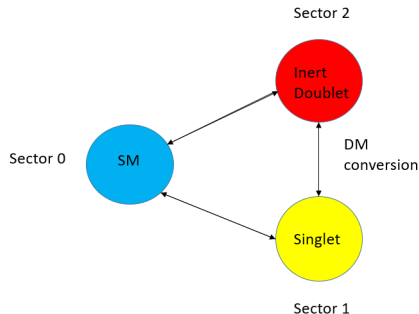
$$\{M_h, M_H, M_A, M_{H^\pm}, M_S, \lambda_2, \lambda_3, \lambda_S, \lambda'_S, \lambda_{S1}, \lambda_{S2}, \lambda_{S12}, \lambda_{S21}\}$$

The remaining parameters of the potential are given by

$$\lambda_1 = \frac{M_h^2}{2v^2} ; \quad \mu_2^2 = M_{H^\pm}^2 - \lambda_3 \frac{v^2}{2} ; \quad \mu_S^2 = M_S^2 - \lambda_{S1} \frac{v^2}{2}$$
$$\lambda_4 = \frac{M_H^2 + M_A^2 - 2M_{H^\pm}^2}{v^2} ; \quad \lambda_5 = \frac{M_H^2 - M_A^2}{v^2}.$$

- DM components are \tilde{S} and \tilde{A} if the pseudo-scalar is stable and do not decay into two singlets.
- We expect similar results if \tilde{H} was the second DM.

The model



- This two DM model provide new types of interactions.
- We call the interaction between the singlet and the doublet "DM conversion".
- Semi-annihilation corresponds to processes that involves two singlets, a doublet and a SM particle.

Relevant trilinear couplings:

- $\lambda_{S1} \rightarrow h\tilde{S}\tilde{S}^\dagger$.
- $-\nu\lambda_{Ah} \rightarrow h\tilde{A}\tilde{A}$, where we introduced $\lambda_{Ah} = \lambda_3 + \lambda_4 - \lambda_5$.
- $-\nu\lambda_{Hh} \rightarrow h\tilde{H}\tilde{H}$, where we used $\lambda_{Hh} = \lambda_3 + \lambda_4 + \lambda_5$.
- $-\nu\lambda_3 \rightarrow h\tilde{H}^+\tilde{H}^-$.
- $\nu(\lambda_{S21} + \lambda_{S12})/2 \rightarrow \tilde{S}\tilde{S}\tilde{H}$.
- $i\nu(\lambda_{S21} - \lambda_{S12})/2 \rightarrow \tilde{S}\tilde{S}\tilde{A}$.

Another relevant coupling would be λ_{S2} . It sets the coupling of the quartic process $\tilde{S}\tilde{S}^\dagger\tilde{A}\tilde{A}$, which contributes to 'DM conversion'.

- Boltzmann equations for \tilde{S} and \tilde{A} ,

$$3H \frac{dY_1}{ds} = \langle v\sigma^{1100} \rangle (Y_1^2 - \bar{Y}_1^2) + \langle v\sigma^{1120} \rangle \left(Y_1^2 - Y_2 \frac{\bar{Y}_1^2}{\bar{Y}_2} \right) + \langle v\sigma^{1122} \rangle \left(Y_1^2 - Y_2^2 \frac{\bar{Y}_1^2}{\bar{Y}_2^2} \right).$$

$$3H \frac{dY_2}{ds} = \langle v\sigma^{2200} \rangle (Y_2^2 - \bar{Y}_2^2) - \frac{1}{2} \langle v\sigma^{1120} \rangle \left(Y_1^2 - Y_2 \frac{\bar{Y}_1^2}{\bar{Y}_2} \right) + \langle v\sigma^{1210} \rangle Y_1 (Y_2 - \bar{Y}_2) + \langle v\sigma^{2211} \rangle \left(Y_2^2 - Y_1^2 \frac{\bar{Y}_2^2}{\bar{Y}_1^2} \right),$$

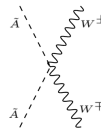
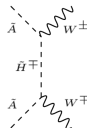
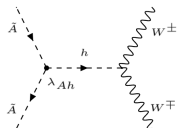
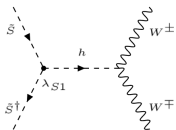
where $Y_{1,2}$ are the abundances of \tilde{S} and \tilde{A} respectively, $\bar{Y}_{1,2}$, the corresponding equilibrium abundances, s is the entropy density and H the Hubble parameter.

- The interaction between the two dark sectors leading to DM conversion and the presence of semi-annihilation terms can strongly affect the relic density of each DM candidate.

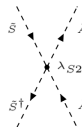
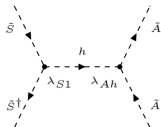
Note that: 0 \equiv SM, 1 \equiv Singlet and 2 \equiv Inert Doublet.

Examples of annihilation processes

$\langle \nu \sigma^{1100} \rangle$ and $\langle \nu \sigma^{2200} \rangle$:



$\langle \nu \sigma^{1122} \rangle$:



$\langle \nu \sigma^{1120} \rangle$ and $\langle \nu \sigma^{1210} \rangle$:

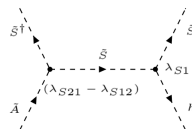
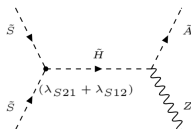
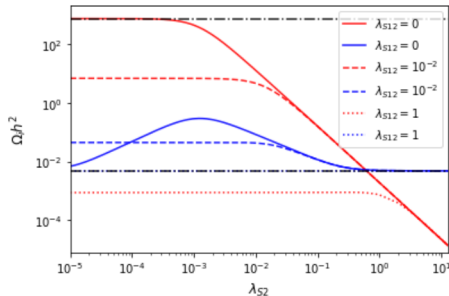


Illustration of the interplay between the two Dark Sectors

- To illustrate the effect of the interactions between the two dark sectors on the relic density of DM, we took an example where we fix $M_A = 120$ GeV, $M_S = 250$ GeV, $M_{H^+} = M_H = 125$ GeV, $\lambda_{S1} = 10^{-3}$ and $\lambda_3 = 8 \times 10^{-3}$ leading to $\lambda_{Ah} = -3.2 \times 10^{-2}$.
- We choose three values for the semi-annihilation couplings $\lambda_{S12} = 0, 0.01, 1$ while always imposing $\lambda_{S12} = -\lambda_{S21}$ to maximize the coupling $\tilde{S}\tilde{S}\tilde{A}$. λ_{S2} is a free parameter.

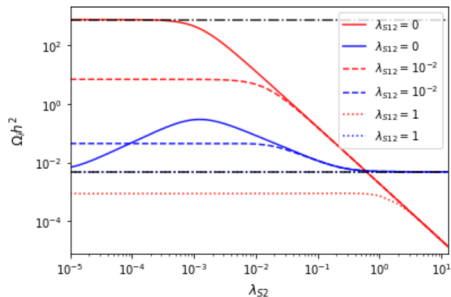
Illustration of the interplay between the two Dark Sectors



$M_A = 120 \text{ GeV}$, $M_S = 250 \text{ GeV}$,
 $M_{H^+} = M_H = 125 \text{ GeV}$,
 $\lambda_{S1} = 10^{-3}$ and
 $\lambda_{Ah} = -3.2 \times 10^{-2}$.

- Red and blue lines corresponds to the relic abundance of \tilde{S} ($\Omega_1 h^2$) and \tilde{A} ($\Omega_2 h^2$) respectively.
- For the choice of parameters, the processes which contribute to DM conversion are driven by λ_{S2} .
- When we neglect semi-annihilation, that is when $\lambda_{S12} = 0$, the relic density of \tilde{S} is very large for $\lambda_{S2} \ll 1$.

Illustration of the interplay between the two Dark Sectors



$$\begin{aligned} M_A &= 120 \text{ GeV}, \quad M_S = 250 \text{ GeV}, \\ M_{H^+} &= M_H = 125 \text{ GeV}, \\ \lambda_{S1} &= 10^{-3} \text{ and} \\ \lambda_{Ah} &= -3.2 \times 10^{-2}. \end{aligned}$$

- $11 \rightarrow 22 \left(\tilde{S}\tilde{S}^\dagger \rightarrow \tilde{A}\tilde{A} \right)$ processes act as additional annihilation channels for \tilde{S} , thus we observe a sharp decrease in Ω_1 for $\lambda_{S2} > 10^{-3}$.
- Because of gauge interactions with the SM, Ω_2 is quite small.
- Turning on the interactions between the dark sector helps increasing Ω_2 . However, when $\lambda_{S2} > 10^{-3}$, these processes become less efficient since Ω_1 decreases sharply.

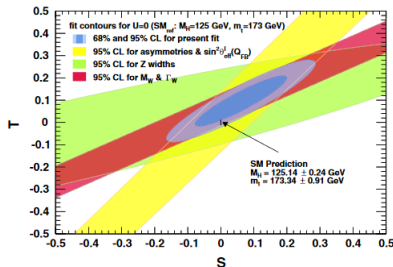
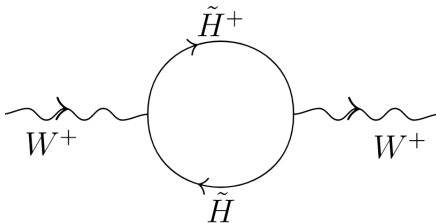
- Perturbativity: the vertex factor for quartic interactions must be smaller than 4π .
- Perturbative Unitarity: For all scalar-scalar scattering processes at high energy, the partial wave unitarity condition should be satisfied for all scattering amplitudes. The eigenvalues of all scattering matrices should be smaller than 8π [*G. Belanger et al. JCAP 06 (2014) 021*].
- Stability conditions of the potential: the quartic potential should be bounded from below.
- Two stable DM candidates: $M_A < 2M_S$.

Collider constraints

- Electroweak precision: S and T are sensitive to physics beyond the SM. In the limit $U=0$

$$S = 0.06 \pm 0.09, \quad T = 0.1 \pm 0.07$$

with a correlation coefficient $+0.91$ [*M. Baak et al. Eur. Phys. J. C 74 (2014) 3046*].



In the low mass region, LEP experiments constraints the parameter space of the model

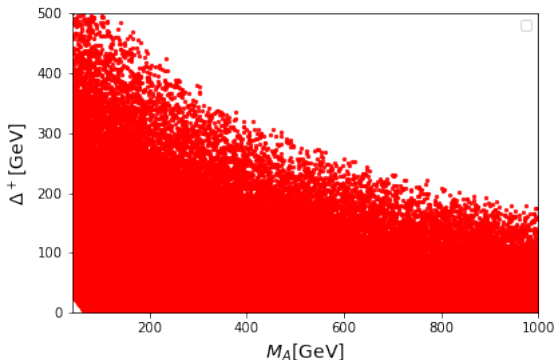
- Widths of W and Z bosons: $W^+ \rightarrow \tilde{H}\tilde{H}^+, \tilde{A}\tilde{H}^+$ and $Z \rightarrow \tilde{A}\tilde{H}, \tilde{H}^+\tilde{H}^-$ should be kinematically forbidden.
- Dijets and di-leptons: The process $e^+e^- \rightarrow \tilde{H}\tilde{A}$ could lead to a visible di-jet or di-lepton signal from $\tilde{H} \rightarrow \tilde{A}\bar{f}f$, a reinterpretation of searches for neutralino pair production in [*E. Lundstrom et al. Phys. Rev. D. 79 (2009) 035013*] rules out:

$$M_A < 80\text{GeV}, \quad M_H < 100\text{GeV}, \quad \text{if } M_H - M_A > 8\text{GeV}$$

- Charged Higgs: The process $e^+e^- \rightarrow \tilde{H}^+\tilde{H}^-$ at LEP2 sets a limit $M_{H^\pm} > 70\text{GeV}$ as a result of the re-interpretation of limits on charginos [*A. Pierce et al. JHEP 08 (2007) 026*].

Collider constraints: LEP

Applying theoretical and LEP constraints leads to an upper limit on the mass difference within the scalar doublet. $\Delta^+ = M_{H^+} - M_A$ should be smaller than about 500 GeV,



For the same reason we need $\Delta^0 = M_H - M_A < 500$ GeV.

- Invisible decay of the Higgs: We use the ATLAS limits obtained in [ATLAS-CONF-2020-052]

$$Br(h \rightarrow \textit{invisible}) < 11\%.$$

- The di-photon decay rate: The charged Higgs contributes to the one-loop induced process $h \rightarrow \gamma\gamma$ decays. (HiggsSignals)
- Finally new physics searches at the LHC allow to probe the model, such as monojet searches, disappearing track (DT) searches, searches for heavy stable charged particles (HSCP) and dileptons.

- Relic density: We require that the total relic $\Omega_{DM}h^2 = \Omega_1h^2 + \Omega_2h^2$ falls within the observed range determined by the PLANCK collaboration within 20% (or 2σ) uncertainty

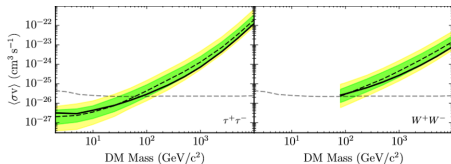
$$0.094 < \Omega_{DM}h^2 < 0.142$$

The relic density and other DM observables are computed using micrOMEGAs.

- Direct Detection(DD): We compute the recoil energy distribution including the two DM signals scaled by their fractional contribution to the total DM density and we use the XENON1T recasted limits at 90% C.L. implemented in micrOMEGAs (*G. Belanger et al. Eur. Phys. J. C 81 no. 3, (2021) 239*).

Dark Matter constraints

- Indirect Detection (ID):
 - FermiLAT observations of photons from Dwarf Spheroidal Galaxies provide one of the most robust constraint on DM especially at masses below the electroweak scale. We compute $\langle v\sigma \rangle$ for $\tilde{A}\tilde{A}$ into WW and ZZ final states and require that their summation lies below the 95% C.L. given by FermiLAT on the WW channel in [*M. Ackermann et al. Phys. Rev. Lett. 115 no.23, (2015) 231301*].



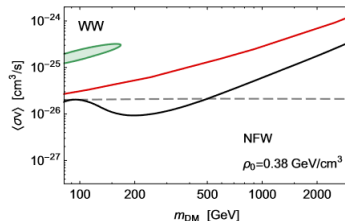
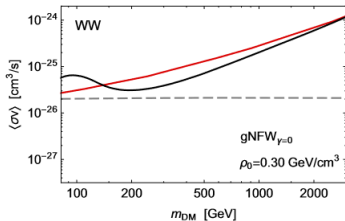
Green: 68% containment
Yellow: 95% containment

Dark Matter constraints

- AMS-02(anti-protons): These constraints strongly depend on the CR propagation parameters as well as on the DM profile. We use the limits derived in [[A. Reinert JCAP 01 \(2018\) 055](#)] from a global fit to B/C ratio and to the anti-proton spectrum. We will consider the fit that is done for two DM profiles,

$$\rho_{DM} = \rho_0 \left(\frac{R_0}{r} \right)^\gamma \left(\frac{R_0 + r_s}{r + r_s} \right)^{3-\gamma}$$

where r_s is the scale radius and γ determines the contraction of the profile.



- XENON-nT and DARWIN: we check the power of future direct detection experiments in constraining the model. We use only a conservative approach where we do not consider the combined signal from both DM particles.
- CTA: Limits on DM annihilation will also be obtained by CTA which measures the photon spectrum albeit at higher energies. We perform a dedicated analysis to determine the parameter space of the model that is within reach of CTA. For this we use the combined photon spectra from all annihilation channels.

Results

- We performed a random scan using a wide range for all the free parameters of the model \rightarrow the general scan
- We used a logarithmic scale for the couplings and a linear scan for the masses and mass splittings (Δ^+ and Δ^0).

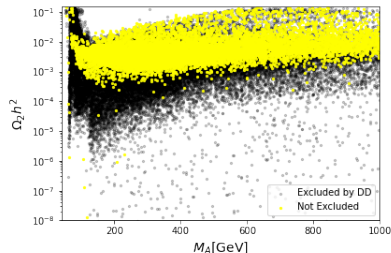
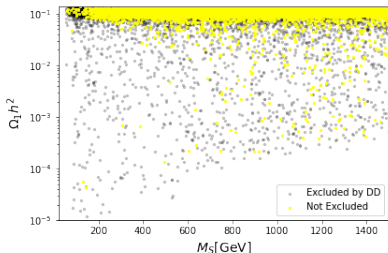
M_A	40 – 1000 GeV	$ \lambda_{S1} $	$10^{-5} - 4\pi$	λ_2	$10^{-5} - 2\pi/3$
Δ^0	0 – 500 GeV	$ \lambda_{S2} $	$10^{-5} - 4\pi$	$ \lambda_3 $	$10^{-5} - 4\pi$
Δ^+	0 – 500 GeV	$ \lambda_{S12} $	$10^{-5} - 4\pi$	λ_S	$10^{-5} - \pi$
M_S	40 – 1500 GeV	$ \lambda_{S21} $	$10^{-5} - 4\pi$	$ \lambda'_S $	$10^{-5} - \pi/3$

Table: Range of the free parameters of the Z4IDSM model used in the scan.

Note that λ_2 , λ_S and λ'_S have no direct impact on the DM phenomenology.

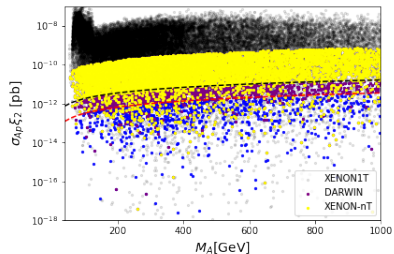
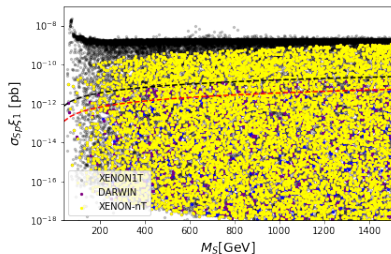
- The relic constraint from PLANCK and the direct detection from XENON-1T provide the most important constraints on the model.
- The role of the LHC is marginal in this scenario. Only the invisible Higgs decay plays some role in the low mass region.

General scan results



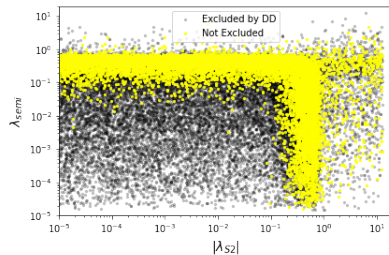
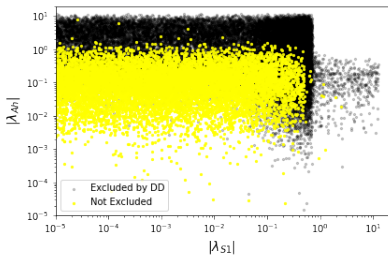
- The singlet forms the dominant DM component most of the time.
- Direct detection limits are satisfied for the full mass range of \tilde{S} above roughly 58 GeV.
- The doublet can only be dominant in a narrow region around $M_h/2$ and for $M_A > 500$ GeV.

General scan results



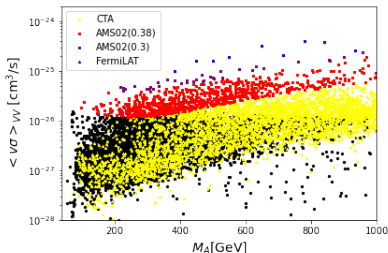
- we show the predictions for the spin independent cross section for each DM candidate over the allowed parameter space. each contribution is rescaled by the appropriate fraction of the DM candidate.
- Even if \tilde{A} is subdominant, it is still effectively probed by XENON1T.
- The singlet component often easily escape DD even if it forms the dominant DM.

General scan results



- $\lambda_{semi} = \sqrt{\lambda_{S12}^2 + \lambda_{S21}^2}$.
- The region where both λ_{semi} and λ_{S2} are small is ruled out by direct detection.
- The bulk of the allowed points are in the region where $0.1 < \lambda_{S2} < 1$ or $0.1 < \lambda_{semi} < 1$.

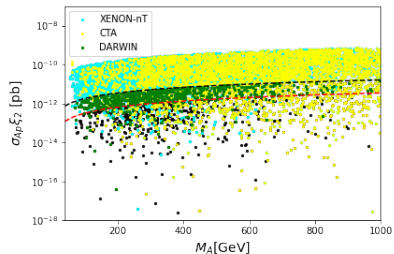
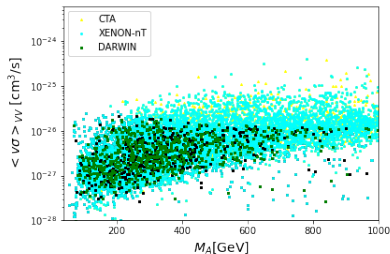
General scan results: indirect detection



- $\langle \nu\sigma \rangle_{VV} = \langle \nu\sigma^{\tilde{A}\tilde{A}WW} \rangle + \langle \nu\sigma^{\tilde{A}\tilde{A}ZZ} \rangle$.
- Black points are out of reach.

- We checked the power of indirect detection to probe the model (photons and anti-protons).
- Large amount of points are within reach of CTA.
- Pair annihilation of \tilde{A} into $W(Z)$ pairs, $\tilde{S}\tilde{S} \rightarrow \tilde{H}^\mp W^\pm$ or processes such as $\tilde{S}\tilde{S} \rightarrow \tilde{H}^+ \tilde{H}^-$ contribute to photon spectrum where $\tilde{H}^+ \rightarrow \tilde{A}, W^+$.

General scan results: Future reach of direct and indirect detection

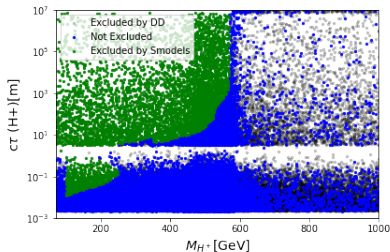


- Large fraction of the points are within reach of both future direct and indirect limits.
- This large overlap between DD and ID opens the possibility of cross-checking a DM signal.
- CTA extend the reach to cases where the doublet is near the TeV scale.

Results: Nearly Degenerate Doublet

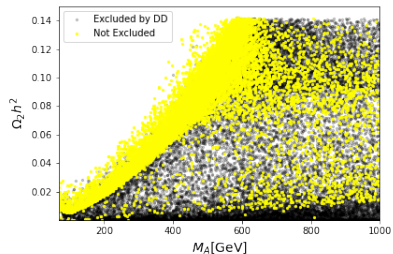
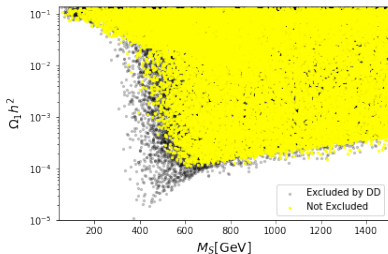
- We performed a dedicated scan for the case of a compressed doublet.
- We considered $\Delta^+ = 1 - 500$ MeV while fixing $\Delta^0 = 201$ KeV.
- \tilde{H} is nearly stable and can be treated as a third DM component.
- $\Omega_{\tilde{H}} \simeq \Omega_{\tilde{A}}$ at the freeze-out temperature.
- The third component will decay into \tilde{A} and will not be present in the Universe today.
- We will use $\Omega_2 = \Omega_{\tilde{H}} + \Omega_{\tilde{A}}$ in what follows.

Results: Nearly Degenerate Doublet



- Charged Higgs (\tilde{H}^+) can be long-lived.
- Dedicated search at the LHC: HSCP and DT searches.
- Heavy stable charged particle searches and disappearing track searches constraints largely the parameter space of the model.

Results: Nearly Degenerate Doublet



- Both the singlet and the doublet can be the dominant DM component.

- Combining the dark matter sectors of the IDM and Singlet model and allowing interactions between the dark sectors opens up significantly the possibility for DM compatible with relic and direct detection constraints.
- Future astrophysics search provide powerful probe of the model.
- While most of the parameter space could be probed, some scenarios escape detection. They correspond to cases where the coupling of DM to the Higgs is suppressed and there is significant amount of semi-annihilation or DM conversion.

Boltzmann Equation For Three DM Components

$$\begin{aligned}
 3H \frac{dY_1}{ds} &= \langle v\sigma^{1100} \rangle (Y_1^2 - \bar{Y}_1^2) + \sum_{k=2,3} \left[\langle v\sigma^{11k0} \rangle \left(Y_1^2 - Y_k \frac{\bar{Y}_1^2}{\bar{Y}_k} \right) \right. \\
 &\quad \left. + \langle v\sigma^{11kk} \rangle \left(Y_1^2 - Y_k^2 \frac{\bar{Y}_1^2}{\bar{Y}_k^2} \right) \right] + \langle v\sigma^{1123} \rangle \left(Y_1^2 - Y_2 Y_3 \frac{\bar{Y}_1^2}{\bar{Y}_2 \bar{Y}_3} \right) \\
 3H \frac{dY_k}{ds} &= \langle v\sigma^{kk00} \rangle (Y_k^2 - \bar{Y}_k^2) + \langle v\sigma^{kk11} \rangle \left(Y_k^2 - Y_1^2 \frac{\bar{Y}_k^2}{\bar{Y}_1^2} \right) \\
 &\quad + \langle v\sigma^{kkk'k'} \rangle \left(Y_k^2 - Y_{k'}^2 \frac{\bar{Y}_k^2}{\bar{Y}_{k'}^2} \right) + \frac{1}{2} \langle v\sigma^{kk23} \rangle \left(Y_k^2 - Y_2 Y_3 \frac{\bar{Y}_k^2}{\bar{Y}_2 \bar{Y}_3} \right) \\
 &\quad + \langle v\sigma^{2300} \rangle (Y_2 Y_3 - \bar{Y}_2 \bar{Y}_3) + \langle v\sigma^{2311} \rangle \left(Y_2 Y_3 - Y_1^2 \frac{\bar{Y}_2 \bar{Y}_3}{\bar{Y}_1^2} \right) \\
 &\quad - \frac{1}{2} \langle v\sigma^{11k0} \rangle \left(Y_1^2 - Y_k \frac{\bar{Y}_1^2}{\bar{Y}_k} \right) + \langle v\sigma^{k110} \rangle (Y_1 Y_k - Y_1 \bar{Y}_k) \\
 &\quad + \Gamma_{kk'} \left(Y_k - Y_{k'} \frac{\bar{Y}_k}{\bar{Y}_{k'}} \right) - \Gamma_{k'k} \left(Y_{k'} - Y_k \frac{\bar{Y}_{k'}}{\bar{Y}_k} \right)
 \end{aligned}$$

Boltzmann Equation For Three DM Components

where $k = 2, 3$, $k' = 5 - k$ and

$$\Gamma_{kk'} = \sum_{\alpha \in k} g_{\alpha} m_{\alpha}^2 \frac{K_1(m_{\alpha}/T)}{\sum_{\beta \in k} g_{\beta} m_{\beta}^2 K_2(m_{\beta}/T)} \Gamma_{\alpha \rightarrow k', SM}^0$$

where $\Gamma_{\alpha \rightarrow k', SM}^0$ is the partial decay width for the decay for one DM into another DM and SM and m_{α} are the DM masses. $K_j(x)$ are the Bessel functions of the second kind and order j .

Effective vertices for $\tilde{H}^\pm \tilde{A} \pi^\mp$ and $\tilde{H}^\pm \tilde{H} \pi^\mp$ interactions

we introduce the non perturbative $W - \pi$ mixing through the Lagrangian

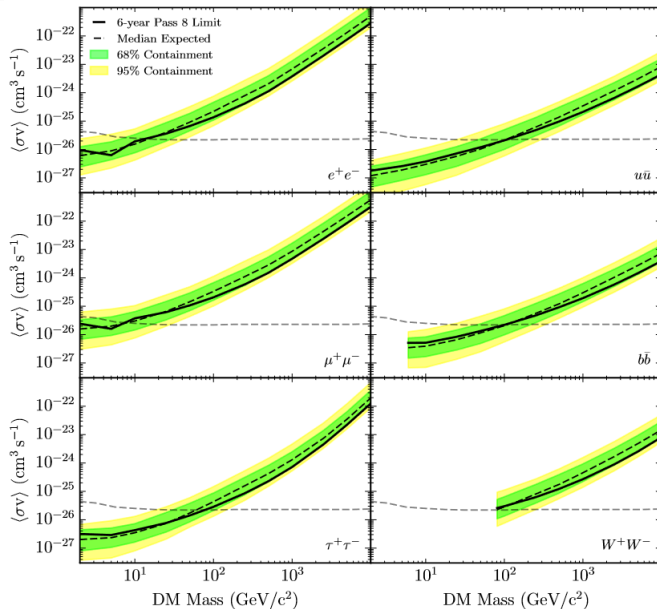
$$\mathcal{L} = \frac{g f_\pi}{2\sqrt{2}} W_\mu^+ \partial^\mu \pi^- \quad (2)$$

such that the $\tilde{H}^+ \tilde{A} \pi^-$ vertex is defined as

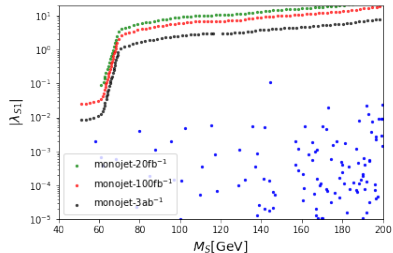
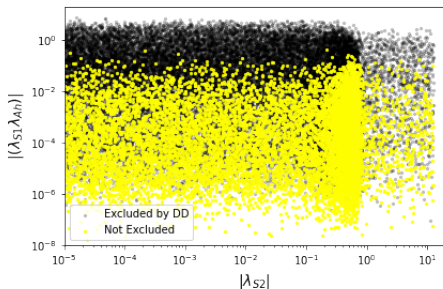
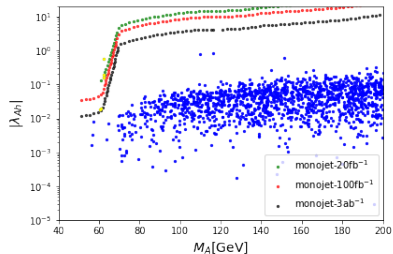
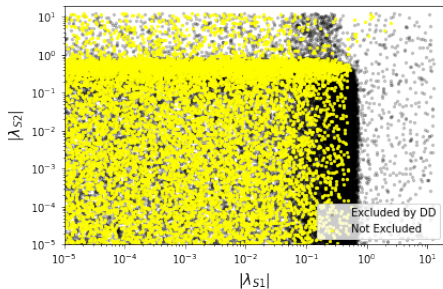
$$\frac{g^2 f_\pi}{4\sqrt{2} M_W^2} (p_{H^+} - p_A) \cdot p_\pi \quad (3)$$

where $f_\pi = 130$ MeV and g is the SU(2) coupling constant. For decays that take place on-mass shell the vertex reduces to $g^2 f_\pi / 4\sqrt{2} (M_{H^+}^2 - M_A^2) / M_W^2$. This effective vertex is taken into account only if Δ^+ lies in the range $140 \text{ MeV} \leq \Delta^+ \leq 500 \text{ MeV}$. For smaller mass splittings the charged Higgs decays into leptons and a neutral Higgs. For larger mass splittings the decay of the charged Higgs is prompt and the decay width into quarks gives an accurate enough result.

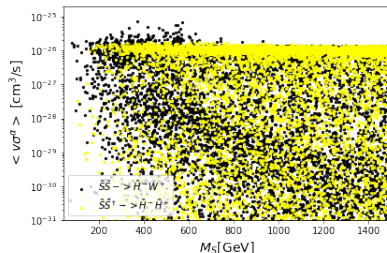
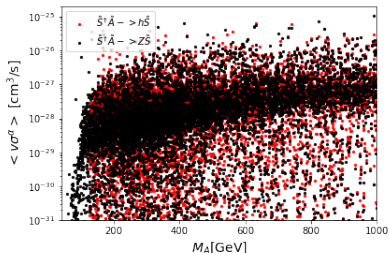
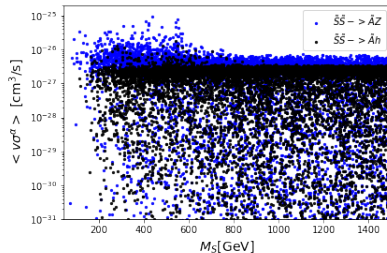
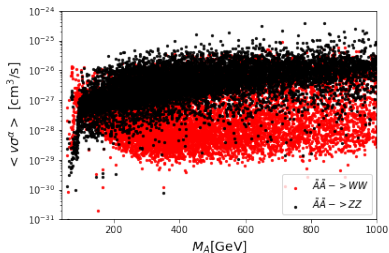
FermiLAT limits all individual channels



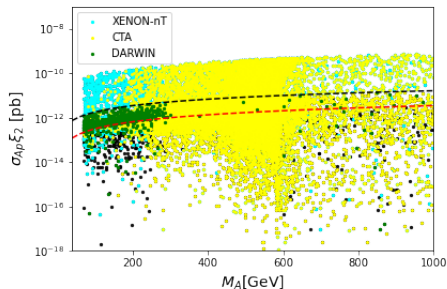
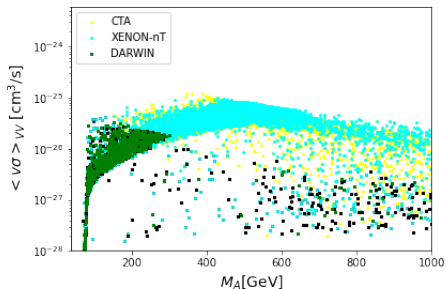
General scan additional plots



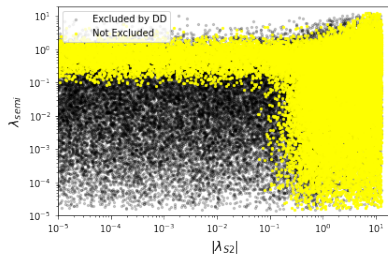
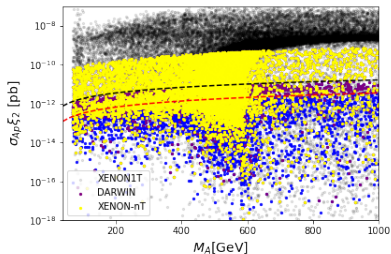
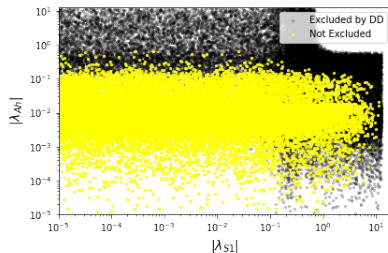
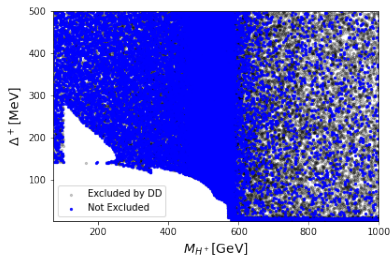
General scan additional plots ID



ND scan results: Future reach of direct and indirect detection



ND additional plots



ND additional plots ID

